Thermomagnetic detection of recrystallization in FeCoNbBCu nanocrystalline alloys

J. S. Blázquez, C. F. Conde, and A. Conde

Citation: Applied Physics Letters **79**, 2898 (2001); doi: 10.1063/1.1413957
View online: http://dx.doi.org/10.1063/1.1413957
View Table of Contents: http://scitation.aip.org/content/aip/journal/apl/79/18?ver=pdfcov
Published by the AIP Publishing

Thermomagnetic detection of recrystallization in FeCoNbBCu nanocrystalline alloys

J. S. Blázquez, C. F. Conde, and A. Conde[a)]
Departamento de Física de la Materia Condensada, Instituto de Ciencia de Materiales, CSIC–Universidad de Sevilla, Apartado 1065, 41080 Sevilla, Spain

(Received 21 June 2001; accepted for publication 20 August 2001)

The recrystallization process in FeCoNbBCu nanocrystalline alloys is evidenced from thermomagnetic results as a significant decrease in magnetization at the second crystallization stage. The lowering in the volume fraction of α-FeCo crystals indicates that some of these crystals contribute to the boride phases formed. Electron microscopy images reveal that the final microstructure consists of large crystals ($\sim$500 nm) of a fcc $(FeCo)_{23}B_6$ phase and small crystals ($\sim$20 nm) of bcc α-FeCo and of some boride phases as such $(FeCo)_2B$. © *2001 American Institute of Physics.* [DOI: 10.1063/1.1413957]

Nanocrystalline soft magnetic materials prepared by primary crystallization of Fe-based amorphous precursors have been extensively studied in the last decade since the report by Yoshizawa[1] on FeSiBCuNb alloys. The microstructure of these composite materials consists of an ultrafine grained ($\sim$10 nm in size) crystalline phase embedded in a residual amorphous matrix. In fact, the small size of the crystallites and their random orientation are responsible for the excellent soft magnetic properties of these two-phase systems.[2] However, an abrupt increase in coercivity of the material is observed at the onset of a second transformation stage, occurring at a higher temperature, that completes the devitrification process with the formation of different boride and niobide phases.

Recently, (Fe,Co)MBCu (M=Nb, Hf, Zr) nanocrystalline alloys, called HITPERM,[3] have been shown to exhibit significantly better high-temperature magnetic properties than in the former FeSiBCuNb (Ref. 1) and FeMBCu (M=Zr, Nb, Hf) (Ref. 4) alloys. Partial substitution of Fe by Co in HITPERM alloys allows us to achieve large induction (1.6–2.1 T), maintained up to higher temperatures, due to the formation of α'-FeCo grains (structure, B2) dispersed in an amorphous phase with a high Curie temperature.

The aim of this work was to investigate nanocrystalline FeCoNbBCu alloys and the study was focused on the structural changes at the second crystallization stage that destroys the nanocrystalline state. In particular, at the onset of this stage a significant decrease in magnetization of the material is observed that evidences a recrystallization process.

For this study, experimental results from differential scanning calorimetry (DSC), thermomagnetic gravimetry (TMG), x-ray diffraction (XRD), and transmission electron microscopy (TEM) have been used. Thermomagnetic curves showing the temperature dependence of the low-field magnetization were obtained in a thermobalance by applying to the sample the magnetic field ($\sim$20 mT) of a small magnet.

For the studied $Fe_{78-x}Co_xNb_6B_{16-y}Cu_y$ ($x=18$, 39, and 60; $y=0$ and 1) alloy series,[5] the crystallization onset, above 700 K, is lowered as the Co content increases and as Cu is introduced. Thermomagnetic measurements on heating show a fall to zero in magnetization M at the ferroparamagnetic transition of the amorphous phase, at about 600 K, followed by an increase in M at the crystallization onset, due to the formation of α-FeCo nanocrystals. The magnetization increases during the nanocrystallization process but above 900 K, at temperatures that coincide with those of the second DSC exotherm, a significant decrease in M is observed although zero magnetization is not reached. This nonzero magnetization remains up to the end of the explored temperature range (1125 K). Figure 1 shows DSC and TMG plots for the $Fe_{60}Co_{18}Nb_6B_{16}$ alloy.

At first sight, the observed decrease in magnetization above 900 K could be assigned to a ferroparamagnetic transition of some phase present at that devitrification stage. The only crystalline phase detected by XRD and TEM is the α-FeCo phase and the amorphous matrix is paramagnetic at these temperatures. However, the temperatures at which this decrease in M occurs are lower than the expected value for the Curie temperature of the FeCo crystals. In fact, for the binary FeCo alloys, the Curie temperature ranges from 1040 to 1200 K, for 0% Co to 15% Co content, and for alloys richer in Co the transition from ferromagnetic bcc FeCo to paramagnetic fcc FeCo (1200–1250 K) occurs below the extrapolated Curie temperature values of the bcc phase.[6] As the

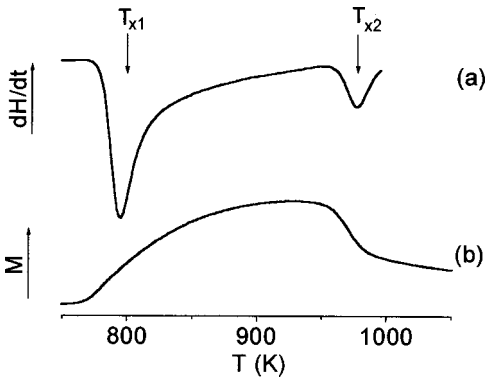

FIG. 1. DSC (a) and TMG (b) plots of the as-cast $Fe_{18}Co_{60}Nb_6B_{16}$ alloy. Arrows indicate the two crystallization peak temperatures.

a)Author to whom correspondence should be addressed; electronic mail: conde@cica.es

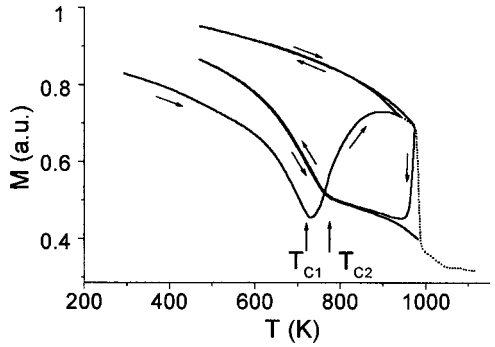

FIG. 2. TMG plot on successive heating–cooling cycles for the $Fe_{39}Co_{39}Nb_6B_{15}Cu_1$ alloy. T_{C1} and T_{C2} indicate the Curie temperature of the amorphous and the $(FeCo)_{23}B_6$ phases, respectively. The-dotted line shows the TMG plot for an as-cast sample in heating up to 1100 K.

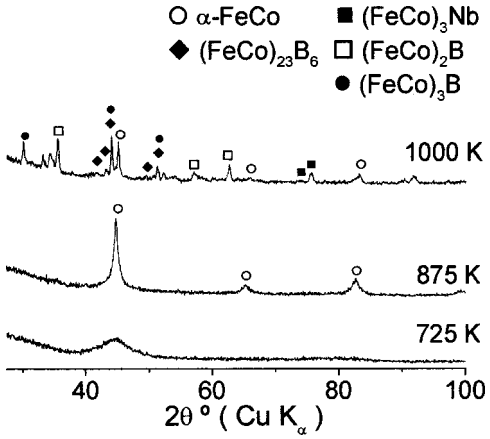

FIG. 3. X-ray diffraction patterns of $Fe_{39}Co_{39}Nb_6B_{15}Cu_1$ alloy samples heated up to the very beginning of the nanocrystallization (725 K), up to the end of the nanocrystallization (875 K), and after the second crystallization process (1000 K).

Curie temperature is an intrinsic property of the material that mainly depends on its composition and structure, the expected value for the Curie temperature of the FeCo nanocrystals would be similar to that for the bulk binary alloy with the same composition. Some experiments have been developed to elucidate the origin of the observed decrease in magnetization at the second devitrification stage, at which the crystallization of the sample is completed with the formation of some boride phases. First, thermomagnetic runs at different heating rates show that the decrease in M corresponds to a thermally activated process: it is shifted to higher temperatures as the heating rate increases, in a similar way as for the increase in magnetization observed at the crystallization onset.

Successive continuous heating and cooling cycles (Fig. 2) show a nonreversible character for the decrease in M, that progresses in each of the repeated heating runs. Another feature observed on the heating–cooling TMG plots is the presence, more evident after each heating run, of a Curie transition-type fall in M at ~775 K, marked as T_{C2} in Fig. 2, that could be associated with the Curie transition of the $(FeCo)_{23}B_6$ phase.[7]

The nonreversible and thermally activated character does not correspond to a Curie transition. A more convincing origin for the observed decrease in magnetization would be a recrystallization process with a lowering of the volume fraction of the magnetic phase (α-FeCo), to form some nonmagnetic phase. From the observation of an enhanced Curie-type fall in M at the expected Curie temperature for the $(FeCo)_{23}B_6$ phase it is easy to infer that some of the FeCo crystals would contribute to the formation of that $(FeCo)_{23}B_6$ phase, and so, the observed progressive decrease in magnetization would be due to a recrystallization process that lowers the volume fraction of the α-FeCo phase.

Structural XRD and TEM results were used to confirm this origin for the decrease in magnetization at the second crystallization stage. Figure 3 shows XRD patterns of $Fe_{39}Co_{39}Nb_6B_{15}Cu_1$ alloy samples heated up to the end of the two crystallization stages. After the primary crystallization only a bcc-FeCo phase coexists with a residual amorphous phase, whereas at the end of the second stage samples are fully crystalline and, along with lines of the α-FeCo phase, x-ray patterns show lines of some boride phases, mainly the $(FeCo)_{23}B_6$ phase. The x-ray patterns of Fig. 3 have been normalized to the same value of the integrated intensity of the total profile and, as observed, the intensities of the α-FeCo lines are smaller for the fully crystalline sample as compared with those for the nanocrystalline sample. A rough estimation of the volume fraction of the α-FeCo phase was done from the ratio of the integrated intensities of this phase profile and the total profile on the angular range 30°–60°. The obtained values are 60% for the nanocrystalline sample and 20% for the fully crystalline sample. This significant decrease in volume fraction of the α-FeCo phase clearly shows that during the secondary crystallization some of the FeCo crystals contribute to the boride phases formed. The decrease of about 2/3 in volume fraction derived from x-ray

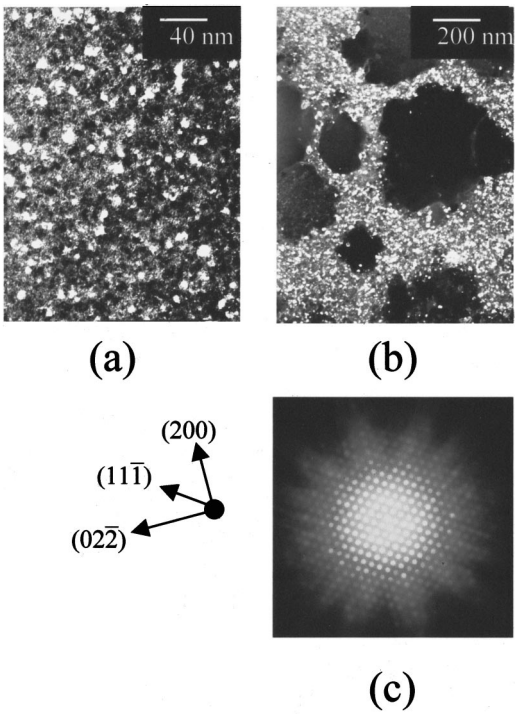

FIG. 4. Dark-field TEM images obtained from the (110) α-FeCo ring for the $Fe_{18}Co_{60}Nb_6B_{15}Cu_1$ alloy: (a) nanocrystalline sample (annealed during 18 000 s at 680 K) and (b) fully crystalline sample (heated up to 900 K). (c) Convergent-beam microdiffraction pattern of the fcc $(FeCo)_{23}B_6$ crystal (zone axis [011]).

data is larger than that observed for M, of about 1/2, but it should be noted that some of the boride phases formed at this stage are ferromagnetic in this temperature range and, therefore, contribute to the M of the material.

Figure 4 shows some TEM results of $Fe_{18}Co_{60}Nb_6B_{15}Cu_1$ samples that evidence the drastic changes in the microstructure occurring at the second stage. At the end of the primary crystallization, a dark-field image [Fig. 4(a)] obtained from the (110) α-FeCo ring shows a homogeneous dispersion of these crystals in the amorphous matrix. The measured mean grain size of 5–10 nm for the $Fe_{18}Co_{60}Nb_6B_{15}Cu_1$ alloy (up to 15–20 nm for other alloys in the series) turns out to be slightly lower than that obtained from x-ray data.[5] After the second crystallization stage, a dark-field image [Fig. 4(b)], also obtained from the (110) α-FeCo ring, shows the coexistence of large crystals, ~500 nm in size, and small crystallites of ~10–20 nm. Convergent-beam microdiffraction [Fig. 4(c)] performed on the large crystals allows us to identify them as the fcc $(FeCo)_{23}B_6$ phase, whereas selected area diffraction patterns show both rings and spots. Rings correspond to the α-FeCo phase and to the different borides, such as $(FeCo)_2B$ and niobides, such as $(FeCo)_3Nb$ phases, found from x-ray patterns, which remain at a small crystal size (~20 nm), whereas the spots can be associated to the large crystals of the $(FeCo)_{23}B_6$ phase. In fact, all the large grains analyzed correspond to the $(FeCo)_{23}B_6$ phase.

In conclusion, the nonreversible and thermally activated process, detected as a decrease in magnetization of the material at the second crystallization stage of the $Fe_{78-x}Co_xNb_6B_{16-y}Cu_y$ studied alloy series corresponds to a recrystallization reaction. The volume fraction of the α-FeCo phase decreases during the formation of the boride phases emerging at this devitrification stage. For the different boride phases formed, the preeminence of the $(FeCo)_{23}B_6$ phase in the volume fraction and with a much coarser grain should be noted.

Work supported by the DGES of the Spanish Ministry of Education (Project No. PB97-1119-C02-01) and by the PAI of the Regional Government of Andalucía (Grant No. FQM 121). One of the authors (J.S.B.) is grateful to the Ministry of Science and Technology for a research fellowship.

[1] Y. Yoshizawa, S. Oguma, and K. Yamauchi, J. Appl. Phys. **64**, 6044 (1988).
[2] G. Herzer, IEEE Trans. Magn. **25**, 3327 (1989).
[3] M. A. Willard, D. E. Laughlin, M. E. McHenry, D. Thoma, K. Sickafus, J. O. Cross, and V. G. Harris, J. Appl. Phys. **84**, 6773 (1998).
[4] K. Suzuki, A. Makino, N. Kataoka, A. Inoue, and T. Masumoto, Mater. Trans., JIM **32**, 93 (1991).
[5] J. S. Blázquez, C. F. Conde, and A. Conde, J. Non-Cryst. Solids **287**, 187 (2001).
[6] A. Fernández-Guillermet, High Temp.-High Press. **19**, 477 (1987).
[7] J. M. Borrego, C. F. Conde, and A. Conde, Philos. Mag. Lett. **80**, 359 (2000).